Can DW-MRI, with its ADC values, be a reliable predictor of biopsy outcome in patients with suspected prostate cancer?

R. Faletti,[1] G. Battisti,[1] A. Discalzi,[1] M. L. Grognardi,[1] S. Martinello,[1] M. Oderda,[2] P. Gontero,[2] L. Bergamasco,[3] M. C. Cassinis,[1] P. Fonio[1]

[1]Radiology Unit, Department of Surgical Sciences, University of Torino, Via Genova 3, 10126 Turin, Italy
[2]Urology Unit, Department of Surgical Sciences, University of Torino, Via Genova 3, 10126 Turin, Italy
[3]Department of Surgical Sciences, University of Torino, Via Genova 3, 10126 Turin, Italy

Abstract

Purpose: To relate the multiparametric magnetic resonance imaging (mp-MRI) of patients with suspect peripheral prostate cancer (PCa) to the results of the subsequent biopsy: in particular to explore whether DWI and ADC can predict the biopsy outcome and to investigate the relation between ADC and Gleason score (GS).

Materials and methods: 175 consecutive patients who underwent 1.5 T mp-MRI followed by prostate biopsy were retrospectively analyzed by two independent radiologists. ADC values were measured in the peripheral suspect lesion areas (ADC_{SL}) and in the contralateral zones (ADC_{NSL}) obtaining $ADC_{norm} = ADC_{SL}/ADC_{NSL}$. Results on T2W images, DWI, ADC values, and perfusion studies were matched to their corresponding biopsy.

Results: Negative DWI and T2W had 100% negative predictive value (NPV). When DWI was positive, $ADC_{SL} > 0.90 \times 10 > 0.90 \times 10^{-3}$ mm^2/s ($ADC_{norm} > 0.60$) identified by the ROC curve (AUC = 0.80) corresponded to NPV = 85%. In positive biopsies, ADC_{SL} and ADC_{norm} decreased significantly from GS = 6 to GS ≥ 8 with Spearman coefficient $\rho = -0.40$ and ROC curve AUC = 0.72.

Conclusion: mp-MRI allows a reliable prediction of a negative biopsy through the values of DWI, T2W, and ADC. In positive biopsies, there is a moderate correlation between ADC and the various GS levels.

Abbreviations

PCa	Prostate cancer
mp-MRI	Multiparametric magnetic resonance
GS	Gleason score
DRE	Digital rectal examination
PBx	Prostate biopsy
DWI	Diffusion-weighted imaging
DCE	Dynamic contrast-enhanced
ADC	Apparent diffusion coefficient
ADC_{SL}	ADC suspicious lesion
ADC_{NSL}	ADC no suspicious lesion
ADC_{norm}	ADC normalized value

Prostate cancer (PCa) is the most commonly diagnosed malignancy of the male genitourinary tract [1]. With the advent of the PSA era, remarkable improvements in its early detection and management have led to a significant increase in the survival rate. On the other hand, the discovery of PCa at its earliest stages spurred questions about the clinical significance of some of these tumors. The balance between the need for early diagnosis and the avoidance of over diagnoses represents a delicate issue, especially if we consider that current recommendations for PCa detection did not change since several years, including PSA level testing, digital rectal examination (DRE), and prostate biopsy (PBx) guided by transrectal ultrasound. These methods, however, have limited accuracy for the majority of early cancers [2] and do not help to clarify the issue about clinically significant PCa.

Correspondence to: R. Faletti; *email:* riccardo_faletti@yahoo.it

In the last years, prostatic multiparametric magnetic resonance imaging (mp-MRI) based on T2-weighted imaging has achieved an important role in the detection and staging of PCa [3]. However, mp-MRI accuracy can be hindered by several factors, including tumor sizes below 5 mm, the seat apical or basal, prostatitis, calcifications, scars, and hemorrhagic foci. Furthermore, the variability in mp-MRI technical features and definitions of PCa clinical significance hamper the comparison of mp-MRI outcomes and its generalization to clinical practice [4]. Keeping in mind these limitations, a promising potential for early PCa detection has been attributed to mp-MRI, when properly used. With the advent of MRI-targeted biopsies, the bioptic detection rate, usually estimated around 33% for standard ultrasound-guided extended biopsy protocols, showed a marked improvement, both in men with previous negative PBx and in naive ones [5, 6].

At present, the most reliable mp-MRI predictors of PCa are functional sequences including diffusion-weighted imaging (DWI) with related apparent diffusion coefficient (ADC), which highlights cell proliferation, and dynamic contrast-enhanced (DCE) imaging for neoangiogenesis. DWI-calculated ADC values of detected lesions were found to have a moderate inverse correlation with the Gleason score (GS), which is the single most important prognostic parameter denoting PCa aggressiveness [7–11]. However, no definitive recommendations were given about the role of mp-MRI in the pre-PBx setting.

We tried to shed light on these issues, of great interest to both radiologists and urologists, by exploring with a retrospective study how negative and positive biopsies are related to mp-MRI parameters. Our scope was to identify the parameters that could help clinicians to decide whether a PBx is actually necessary, and if this is the case, to aim the biopsy on the most significant lesions.

Materials and methods

Study population

The study population was extracted from 525 consecutive patients who underwent prostatic MRI in our facility between January 2011 and December 2014. All patients had suspicion of PCa, due to elevated PSA, positive DRE, and/or transrectal ultrasound findings.

We considered only patients whose suspicious lesion was identified by MRI in the peripheral zone and underwent PBx within 3 months after MRI.

Exclusion criteria were findings of multifocal bilateral neoplastic areas at subsequent PBx (in order to obtain a good correlation between the mp-MRI suspected area and biopsy), and a recent previous PBx (to avoid the risk that post-biopsy hemorrhage might determine artifacts on DWI and ADC map). The final number of patients thus amounted to 175.

All patients signed an informed consent form and the study was conducted in good clinical practice according to the Helsinki Declaration of 1975 and subsequent modifications.

MRI protocol

MRI was performed on a 1.5 T superconductive magnet system (Achieva version 2.6; Philips Medical Systems, DA Best, Netherland) consistent with the Consensus Conference of the European Association of Urology [12]. We followed the ESUR (European Society of Urogenital Radiology) prostate MR guidelines of 2012 [13], using the cardiac 32-channels surface coil (pelvic phased-array coil PPA) instead of the endorectal coil (ERC), which has recognized drawbacks in terms of cost and patient acceptability. If tolerated, a 1 mg Hyoscinbutylbromide (Buscopan, BoehringerIngelheim, Ingelheim am Rhein, Germany) intravenous injection was administered to the patient to reduce peristaltic motion.

ADC map was automatically reconstructed on a pixel-by-pixel basis ($b = 0$ and 1500 s/mm^2). The examination was completed with high-temporal resolution DCE imaging with Gradient-echo (GRE) axial fast 3D T1-weighted fat suppression sequence (started after) and intravenous administration of 0.1 mmol/kg at a rate of 3.0 mL/s of Gadobenic acid (Gd-BOPTA, Multihance®, Bracco Corporates, Italy), followed by a 20-mL saline flush at the same infusion rate. Approximately, 40 sets of images were acquired to monitor the time course of the contrast agent uptake and clearance within the prostate.

The main features of the study protocol are summarized in Table 1.

Imaging analysis

Image evaluation was performed using a medical imaging workstation (MR Extended Work Space 2.6.3.2 2009 software, Philips Medical Systems, Eindhoven, The Netherlands).

Two observers (R.F. and G.B., with 5 and 3 years experience in prostate MR imaging) reviewed and evaluated qualitatively all images (DWI, T2W and DCE) in a randomized and blinded way; for DWI images, they also measured the corresponding ADC values both in the suspicious lesion (SL) peripheral area and in the contralateral peripheral zone with no suspicious lesions (NSL). We considered only tumors in the peripheral prostate because ADC is significantly different for tumors occurring in the transitional zone compared to the peripheral zone.

A lesion was considered suspicious when it had (i) clear definition (≥5 mm); (ii) low signal intensity on T2W with restricted diffusion; (iii) hypointensity on the ADC map; and (iv) intense early enhancement and rapid

Table 1. mp-MRI protocol of our study

Parameters	T2W axial	T2W sagittal	T2W coronal	DWI	DCE
Section Thickness/gap (mm)	3/0	3/0	3/0	3/0	3/0
Phase-encoding direction	Right to left	Foot to head	Right to left	Anteroposterior	Anteroposterior
Repetition time (ms)	4157	5214	4615	4061	4,7
Echo time (ms)	100	100	100	74	2,3
Field of view	$180 \times 180 \times 66$	$180 \times 86 \times 180$	$180 \times 180 \times 76$	$180 \times 243 \times 69$	$231 \times 80 \times 80$
Acquisition matrix	256×198	256×204	256×198	80×94	100×129
Acquired voxel size	0.7×0.88	0.7×0.88	0.7×0.88	2.25×2.5	$1.8 \times 2 \times 1.8$
Reconstructed voxel size	0.469	0.469	0.469	1.41	1
b Values (s/mm^2)				0–1500	
No. of repetition	4	3	4	6	1
Turbo factor	18	18	18	50	
Acquisition duration (min)	3	3	3	4	5
Flip angle (degrees)	90	90	90	90	10

washout on DCE. These features correspond to a most probably malignant (PI-RADS 5) on PI-RADS classification [14].

Suspect hypointense areas on T2W were searched on DWI sequences; when confirmed, a ROI (region of interest) was drawn manually on the ADC map over the center of the suspect zone, excluding the tumor edges. We used the ROI drawn on the T2W dataset instead than on the DWI one, because of the significantly better spatial resolution of the former. The suspicious lesion ROI was automatically converted from the ROI on T2W images to DCE-MRI using image-registration software. The area of ROIs ranged from 5 to 18 mm^2 due to the wide range in size of prostate glandes and PCas. The information on the contralateral peripheral parenchyma, cancer-free according to the histological report, was obtained by drawing a ROI with size from 5 to 20 mm^2 on the same image of the suspicious lesion.

Based on the brightness of the color-coded value of each parameter, the outcome of the mp-MRI exam was summarized for each patient as follows: T2W = 0 or 1, with 1 standing for predominantly distinctly hypointense compared to the hyperintense glandular tissue of the peripheral zone, DWI = 0 or 1, with 1 standing for strongly and focal signal increment. When DWI = 1 and/or T2W = 1, there was also the information on the ADC value and on DCE = 0 or 1, with 1 standing for a curve with immediate washout after peak enhancement [15].

Prostate biopsy protocol

All ultrasound-guided biopsies were performed by experienced urologists. An extended 12-core template was followed, as recommended by European Association of Urology guidelines [16]. Dedicated uro-pathologists experienced in urogenital diseases were responsible for all histopathologic reports. Gleason score was attributed according to the 2005 International Society of Urological Pathology (ISUP) [17]; in case of more than one positive cores, the Gleason score considered was the highest found.

Statistical analysis

Continuous variables were checked for normality with Kolmogorov–Smirnov–Lilliefors test, D'Agostino test, and the Shapiro–Wilk W test. Since no evidence against normality was found, they were reported as mean ± standard deviation. Statistically significant differences among $k = 2$ independent distributions were investigated with Student t test and double-checked with Mann–Whitney's test (age, PSA and ADC in positive and negative biopsies): for $k > 2$ with ANOVA and Kruskal–Wallis's test (ADC for different GS grades). The relation between a bivariate set of paired continuous xy rankings was explored with Spearman's rank correlation coefficient ρ with its relative p ($\rho = o$).

Binary variables, reported as counts and percentages, were arranged in 2×2 tables studied with the Chi-square test with Yates' correction and Fisher exact test, estimating also the odds ratio (OR) with its 95% confidence interval (CI).

Statistical significance was set at two-tails $p < 0.05$ and OR 95% CI's not including 1.

Inter-reader agreement was assessed in different ways for qualitative and quantitative analysis. For the former we used Cohen's coefficient kappa (<0.20, poor agreement; 0.21–0.40 fair; 0.41–0.60 moderate; 0.61–0.80 good; 0.81–1.00 excellent). Agreement on ADC reading was determined with the Student test for 2 correlated distributions and the non-parametric Wilcoxon's test: $p > 0.05$ implies the absence of statistically significant differences between the two readers, the absence which gets more and more important up to $p = 1$ (lack of differences, perfect agreement on the ADC value).

ADC discrimination ability was assessed by the receiving operating characteristics (ROC) curve, and the quality of discrimination was measured by the area under the curve (AUC), 0.5 being null (chance) and then increasing from 0.6 (poor) to 1 (excellent). The threshold disease/not disease was set at the value which maximized the harmonic mean (HM) of sensitivity and specificity, Jouden's index J, Cohen's kappa, and diagnostic accu-

racy and also minimized the distance D of the curve from the (0,1) upper left vertex.

Open source software (www.openepi.com and www.vassarstats.net) and Statplus:Mac version v6 (AnalystSoft, Walnut, CA, US) were used along with Excel spread sheets. All statistical procedures were run on at least two different packages.

Results

The consensus on the imaging analysis between the two readers was very good in both qualitative analysis (Cohen's concordance coefficient $k = 0.94 \pm 0.2$) and on the measured ADC values ($p = 0.89$).

Each patient was described by the parameters of his mp-MR examination (T2W, DWI, ADC values and DCE) and the outcome of his biopsy (negative/positive; in the latter case with the reported GS). Table 2 reports the descriptive parameters of patients. Patients negative at PBx were successively followed-up with regular clinical visits comprehensive of PSA measurement and DRE, for 19.4 ± 1.7 months.

DWI = 0 and T2W = 0 characterized 43/104 (41%) patients with negative biopsies and no patients with positive biopsies ($p < 0.0001$).

DWI = 1 characterized 61/104 (59%) patients with negative biopsies and all 71 (100%) patients with positive biopsies. These 132 patients constituted the sample considered for ADC and DCE analysis.

Table 3 reports the average ADC values measured in the SL and NSL peripheral areas. The former were significantly lower for patients with positive biopsies than for patients with negative biopsies, whereas the latter were quite similar; in both cases, ADC_{SL} was significantly lower than ADC_{NSL}. The computation of the ratio

$ADC_{norm} = ADC_{SL}/ADC_{NSL}$ had the double purpose of evening out biological differences within patients and allowing comparisons with other studies.

The ROC curve procedure assessed the ability of ADC_{SL} to discriminate between suspicious lesions confirmed as tumors and those negative at biopsy. The top panel of Fig. 1 shows the ROC curves relative to ADC_{SL} and ADC_{norm}, which share the value of AUC = 0.80 (95% CI 0.70–0.90). The bottom panel of Fig. 1 shows that both ROC curve parameters HM and k have their maximum at $ADC_{SL} = 0.90 \times 10^{-3}$ mm^2/s, which is
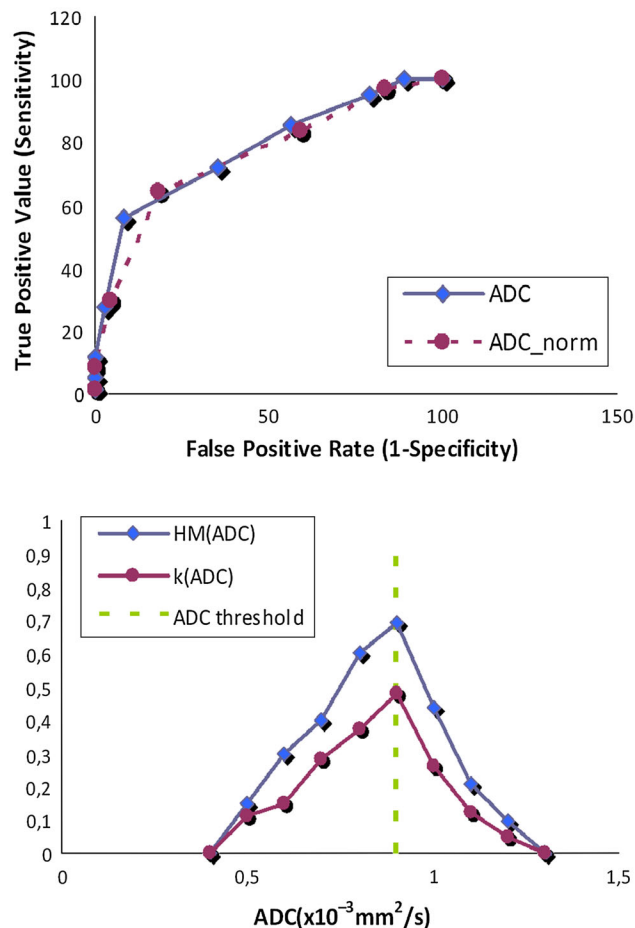

Fig. 1. ROC procedure to estimate the ADC ability to discriminate between negative and positive biopsies. *Top panel* ROC curves for ADC_{SL} and ADC_{norm} (AUC = 0.80). *Bottom panel* Determination of the threshold ($ADC_{SL} = 0.9 \times 10^{-3}$ mm^2/s).

Table 2. Descriptive parameters of patients enclosed in the study

	Positive biopsies	Negative biopsies	p
N	71	104	
Age	67.8 ± 9.2	64.5 ± 7.0	0.005
PSA	11.4 ± 11.0	7.6 ± 5.9	0.02
GS 6(3 + 3)	15		
GS 7(3 + 4)	30		
GS 7(4 + 3)	17		
GS 8(4 + 4)	4		
GS 9(4 + 5)	4		
GS 9(5 + 4)	1		

Table 3. Patients with DWI = 1 ($N = 132$): apparent diffusion coefficient ($\times 10^{-3}$ mm^2/s) in negative and positive biopsies

	Negative biopsies (61)	Positive biopsies (71)	p (neg vs. pos)
No suspicious lesion: ADC_{NSL}	1.55 ± 0.16	1.56 ± 0.21	0.41
Suspicious lesions ADC_{SL}	0.91 ± 0.17	0.72 ± 0.16	<0.0001
p (ADC_{NSL} vs. ADC_{SL})	<0.0001	<0.0001	
$ADC_{norm} = ADC_{SL}/ADC_{NSL}$	0.59 ± 0.13	$0.47 \pm 0.11(0.44–0.50)$	<0.0001

thus identified as the threshold above which there is the highest degree of association with negative biopsies. The corresponding diagnostic parameters are 60% sensitivity, 92% specificity, and 75% diagnostic accuracy.

The domain characterized by $ADC_{SL} > 0.90 \times 10^{-3}$ mm^2/s includes 40 patients, 34 (85%) with negative biopsies and 6 (15%) with positive biopsies, 4 of them GS6, and 2 GS 7(3 + 4). The complementary domain $ADC_{SL} \leq 0.90 \times 10^{-3}$ mm^2/s includes 92 patients, 65 (71%) with positive biopsies and 27 (29%) with negative biopsies ($p < 0.0001$).

The incidences of the mp-MRI parameters in negative and positive biopsies are reported and are compared in Table 4. Their relative OR 95% CIs are plotted in the forest plot of Fig. 2. No 95% CI includes 1, evidencing a significant association either with negative biopsies or with positive biopsies; the farther from 1 the OR 95% CI, the strongest the association.

A similar procedure identifies 0.6 as the corresponding threshold for ADC_{norm}.

It is well known that both the average ADC_{SL} and ADC_{norm} in positive biopsies are influenced by the inci-

dence of the different Gleason scores. In our study, GS ranged from 6(3 + 3) to 9(5 + 4), as detailed in Tables 1 and 5. Figure 3 shows how ADC_{SL} has a significant moderate inverse correlation with GS: Spearman's rank correlation coefficient is $\rho = -0.40$, with p $(\rho = 0) = 0.001$, consistent with the statistically significant decrease of ADC_{SL} and ADC_{norm} ($p = 0.014$).

The previous results are confirmed by the ROC curve procedure: AUC = 0.72 for the ability of ADC_{SL} and ADC_{norm} to identify GS > 6 levels, with thresholds $ADC_{SL} \leq 0.70 \times 10^{-3}$ mm^2/s and $ADC_{norm} \leq 0.50$.

Figure 4 shows the sequences relative to one case with negative mp-MRI and three cases with positive mp-MRI and biopsies corresponding to two GS values.

Discussion

Our study showed that DWI = 0 and T2W = 0 were associated with negative biopsies for all our patients. DWI evaluates differences in water molecule diffusion by qualitative visual assessment using relative signal intensity and also by quantitative assessment by calculating

Table 4. Incidence of mp-MRI parameters

	Negative biopsies	Positive biopsies	p	OR
DWI = 0				
N = 43				
T2W = 0	43/104 (41%)	0/71 (0%)[a]	<0.0001	<0.02 (0.03–0.15)
DWI = 1				
N = 132				
T2W = 0	13/61 (21%)	13/61 (21%)	0.0006	0.005 (0.007–0.4)
T2W = 1	48/61 (79%)	71/71 (100%)[a]	0.0006	>19 (2.4–150)
DCE = 1	35/61 (57%)	57/70[b] (81%)	0.005	3.3 (1.5–7)
$ADC_{SL} \leq 0.90$	27/61 (44%)	65/71 (92%)	<0.0001	13.3 (5–39)
T2W = 1+DCE = 1	25/61 (41%)	57/70 (81%)	<0.0001	6.3 (3–14)
T2W = 1 + $ADC_{SL} \leq 0.90$	22/61 (36%)	65/71 (92%)	<0.0001	19 (7–51)
T2W = 1 + $ADC_{SL} \leq 0.90$ + DCE = 1	11/61 (18%)	53/70[b] (76%)	<0.0001	14 (6–37)

[a] Computed as 70/71 since some calculations are not possible with a zero cell
[b] One DCE value is missing among the positive biopsies patients because of technical problems during the exam
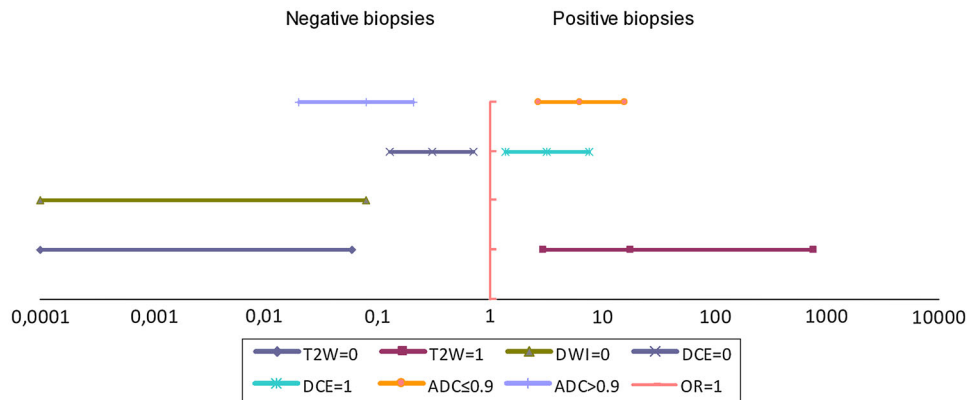

Fig. 2. Forest plot with mp-MRI predictors of negative or positive biopsies. The intervals represent the odds ratio 95% CIs, on a logarithmic scale. OR intervals <1: significant association with negative biopsies; OR intervals >1: significant association with positive biopsies.

the ADC. Because of the many tightly packed glandular elements with little central space for mucin or fluid storage in prostate cancer, ADC values, which corre-
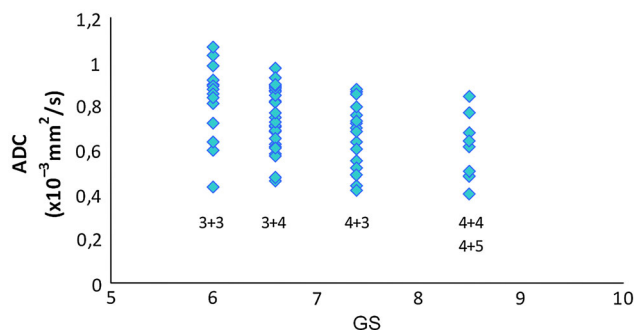

Fig. 3. ADC_{SL} plotted as a function of the Gleason score (Spearman's $\rho = -0.40$).

spond to the restriction of water displacement, are reported significantly lower than in normal prostates [11]. Although ADC represents capillary perfusion and diffusion characteristics, the use of a large b value can reduce the influence of capillary perfusion. Proton diffusion properties of water in high b value with increased signal to noise ratio (SNR), diffusion-weighting, and diminished T2 shine-through may reflect the cellular density and structural changes in prostate cancer more strongly than in standard b value in DWI. On the other hand, a b value > 2000 induces a decrease in SNR and an increase in susceptibility artifacts and image distortion [18].

The finding of NPV = 100%, with 95% CI probability of having a positive biopsy 0–5%, is in agreement with recent works [19–21]. If confirmed in larger data-
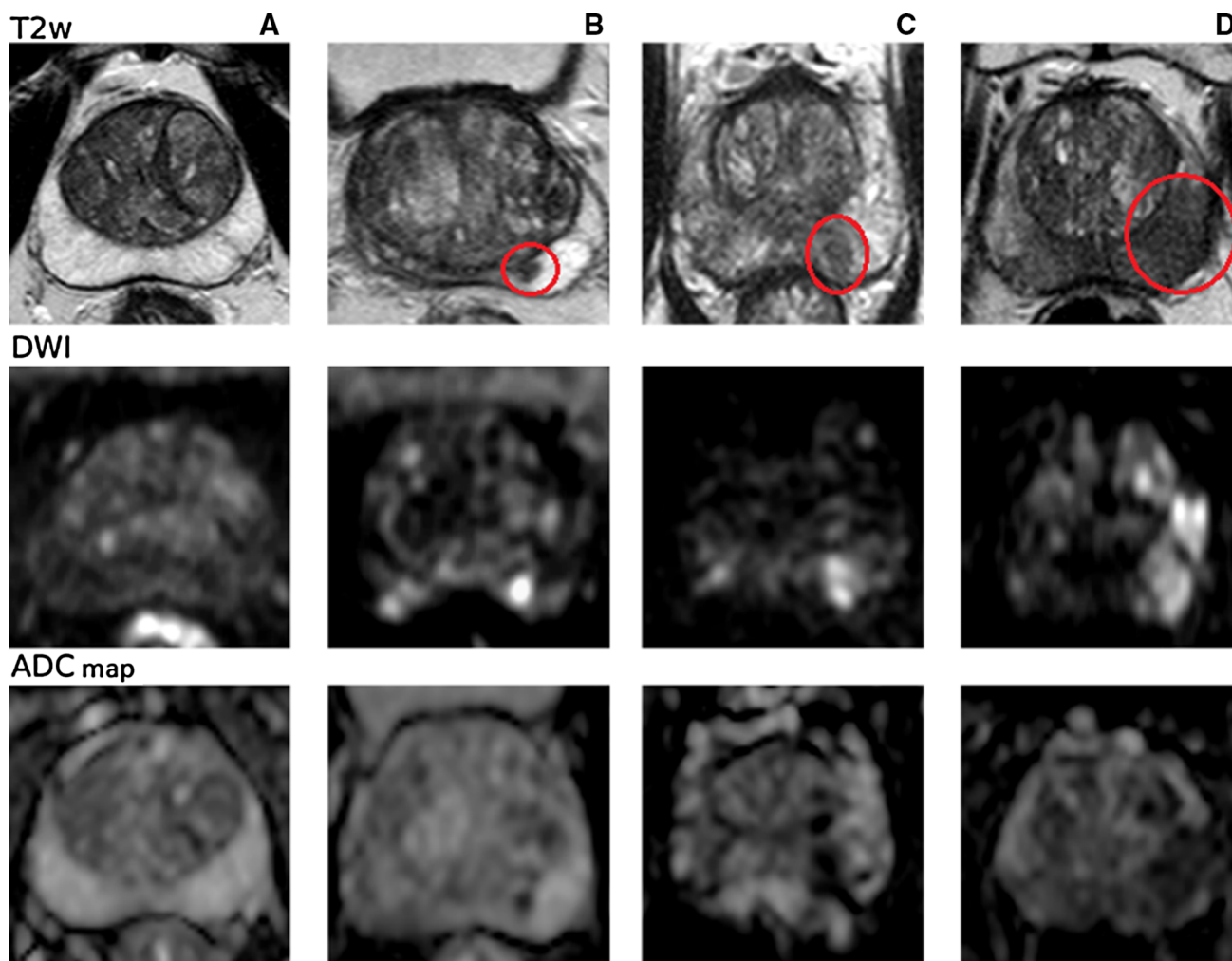

Fig. 4. mp-MRI sequences of four typical cases (T2W, DWI, and ADC map): **A** patient with negative MRI diagnoses ($ADC_{NSL} = 1.61 \times 10^{-3}$ mm^2/s); **B** patient with positive mp-MRI (left posterolateral base nodule) and positive biopsy with GS = 6 ($ADC_{SL} = 0.85 \times 10^{-3}$ mm^2/s; $ADC_{norm} = 0.54$); **C** patient with positive mp-MRI (left posterolateral paramedian focal lesion) and positive biopsy with GS = 7(3 + 4) ($ADC_{SL} = 0.75 \times 10^{-3}$ mm^2/s; $ADC_{norm} = 0.48$); and **D** patient with positive mp-MRI (left posterolateral middle wide lesion) and positive biopsy with GS = 9(5 + 4) ($ADC_{SL} = 0.60 \times 10^{-3}$ mm^2/s; $ADC_{norm} = 0.38$).

Table 5. Patients with positive biopsies ($N = 71$): mp-MRI parameters for different GS

GS	N	ADC$_{SL}$ ($\times 10^{-3}$ mm^2/s)	ADC$_{NSL}$ ($\times 10^{-3}$ mm^2/s)	ADC$_{norm}$	DCE = 1[a]
6(3 + 3)	15	0.82 ± 0.17(0.73–0.91)	1.57 ± 0.09(1.54–1.64)	0.53 ± 0.11(0.47–0.58)	10/15
7(3 + 4)	30	0.74 ± 0.13(0.69–0.79)	1.55 ± 0.20(1.48–1.62)	0.47 ± 0.09(0.44–0.51)	24/29[a]
7(4 + 3)	17	0.68 ± 0.14(0.61–0.75)	1.54 ± 0.25(1.41–1.67)	0.44 ± 0.09(0.39–0.48)	15/17
≥8	9	0.63 ± 0.14(0.52–0.74)	1.47 ± 0.15(1.35–1.59)	0.40 ± 0.09(0.33–0.47)	8/9
p		0.009	0.53	0.009	0.38

[a] One DCE value is missing because of technical problems during the exam
[b] GS8(4 + 4), GS9(4 + 5), and GS9(5 + 4) were grouped together because of their low sample sizes

sets, this result would be an important achievement, as up-to-date, in the presence of PCa clinical suspicion, a PBx is advised irrespectively of MRI findings. However, this association should be tested in more extreme situations, such as patients with very high levels of PSA or frankly positive DRE, to verify if it is still safe to avoid a PBx also in these cases.

As for ADC, in the presence of signal increment, DWI-calculated ADC$_{SL}$ values in suspicious areas were significantly different between positive and negative PBx, with no overlapping of the relative 95% CIs 0.87–0.95 $\times 10^{-3}$ mm^2/s for the former and 0.68–0.76 $\times 10^{-3}$ mm^2/s for the latter. On the contrary, in the NSL zones, the ADC values were similar for negative and positive biopsies, with average value 1.56 ± 0.21 $\times 10^{-3}$ mm^2/s, consistent with other studies with similar b values: 1.48 ± 0.29 for Woodsfield [22], 1.60 ± 0.25 for Hambrock [23], and 1.79 ± 0.28 for Tamada with $b = 0$–1000 and 1.32 ± 0.24 with $b = 0$–2000 [18].

The ROC curve procedure allowed to associate the region of ADC$_{SL}$ > 0.9 $\times 10^{-3}$ mm^2/s to an 85% probability of negative biopsies, presumably with a scant probability of histological presence of cancer. For ADC$_{norm}$ = ADC$_{SL}$/ADC$_{NSL}$, the corresponding threshold was 0.60. To test its general applicability, we considered results obtained in other studies. Again, the wide variability in mp-MRI technical features (field strength, coils, highest b values) and clinical factors (GS distribution, cancer, and cancer-free zones considered) allowed only rough comparisons [4]. Recent studies with technical characteristics not too different from ours reported for ratio of ADC between cancerous and not-cancerous regions ≈0.54 for Tanimoto [24], ≈0.50 for Woodfield [22], ≈0.53–0.55 for Tamada [18], and ≈0.49 for Boesen [25]. Despite the heterogeneity of these studies, all figures satisfy the threshold ADC$_{norm}$ > 0.60 as indicator of benignity.

In patients where PCa was found at biopsy, our study confirmed the existence of a moderate inverse correlation between ADC$_{SL}$ and GS, measured by $\rho = -0.40$, midway between the values −0.50 by Tamada [18] and −0.42 by Boesen [25], and the values −0.38 by Thormer [26] and −0.37 by Oto [3]. Also, a significant ADC decrease was detected from GS = 6 to GS ≥ 8.

The ADC$_{norm}$ ≤ 0.50 threshold for GS > 6 suggested by the ROC curve accounts for the data by Woodfield [22] (≈0.45), Boesen [25] (≈0.46), Thörmer [26] (≈0.46), and Tamada [18] (≈0.49–0.51). It is important to notice that all these studies refer to GS measured after prostatectomy.

DCE = 0 was a significant predictor of negative biopsies, even if to a minor degree than DWI = 0 and ADC > 0.90 $\times 10^{-3}$ mm^2/s. In positive biopsies, DCE = 1 did not contribute significantly to the GS stratification ($p = 0.40$).

Our study is affected by the limitations deriving from its retrospective nature.

Needle biopsies are known to underestimate GS in approximately 25% of the cases compared with prostatectomy specimens because of biopsy sampling errors and tumors heterogeneity [3]. Furthermore, in our series, biopsies were performed with visual registration, the so-called "cognitive" approach, as at the time of study enrollment a mpMRI/ultrasound fusion device was not available at our institution. Therefore, we have to consider a non-negligible percentage of human error typical of cognitive approach. As for standard, extended PBx, a 20% of false negatives has to be taken into account, considering that, even in positive cases, some cancer foci may be missed by the biopsy.

All that considered, our results suggest that mp-MRI has the potential for becoming a first-line examination in patients with clinical suspicion of peripheral PCa. Negative MRI findings, including DWI = 0, T2W = 0, and ADC$_{norm}$ values >0.60, might spare unnecessary PBx, at least in patients not at very high clinical PCa risk. On the other hand, a strong MRI suspicion should not be ignored, particularly if ADC$_{norm}$ falls below 0.5, prompting a targeted biopsy if possible.

subsequent modifications.Written informed consent was obtained from all patients in this study.

References

1. Min BD, Kim WT, Cho BS, et al. (2012) Usefulness of a combined approach of t1-weighted, t2-weighted, dynamic contrast-enhanced, and diffusion-weighted imaging in prostate cancer. Korean J Urol 53:830–835. doi:10.4111/kju.2012.53.12.830
2. Kitamura K, Muto S, Yokota I, et al. (2014) Feasibility of multi-parametric prostate magnetic resonance imaging in the detection of cancer distribution: histopathological correlation with prostatectomy specimens. Prostate Int 2:188–195. doi:10.12954/PI.14067
3. Oto A, Yang C, Kayhan A, et al. (2011) Diffusion-weighted and dynamic contrast-enhanced MRI of prostate cancer: correlation of quantitative MR parameters with Gleason score and tumor angiogenesis. AJR Am J Roentgenol 197:1382–1390. doi:10.2214/AJR.11.6861
4. Fütterer JJ, Briganti A, De Visschere P, et al. (2015) Can clinically significant prostate cancer be detected with multiparametric magnetic resonance imaging? A systematic review of the literature. Eur Urol. doi:10.1016/j.eururo.2015.01.013
5. Schoots IG, Petrides N, Giganti F, et al. (2015) Magnetic resonance imaging in active surveillance of prostate cancer: a systematic review. Eur Urol 67:627–636. doi:10.1016/j.eururo.2014.10.050
6. Valerio M, Donaldson I, Emberton M, et al. (2014) Detection of clinically significant prostate cancer using magnetic resonance imaging–ultrasound fusion targeted biopsy: a systematic review. Eur Urol. doi:10.1016/j.eururo.2014.10.026
7. Haghighi M, Shah S, Taneja SS, Rosenkrantz AB (2013) Prostate cancer: diffusion-weighted imaging versus dynamic-contrast enhanced imaging for tumor localization-a meta-analysis. J Comput Assist Tomogr 37:980–988. doi:10.1097/RCT.0b013e3182a3f9c7
8. Panebianco V, Barchetti F, Manenti G, et al. (2015) MR imaging-guided prostate biopsy: technical features and preliminary results. Radiol Med 120:571–578. doi:10.1007/s11547-014-0490-0
9. Zhang Y-D, Wang Q, Wu C-J, et al. (2015) The histogram analysis of diffusion-weighted intravoxel incoherent motion (IVIM) imaging for differentiating the gleason grade of prostate cancer. Eur Radiol 25:994–1004. doi:10.1007/s00330-014-3511-4
10. Schimmöller L, Quentin M, Arsov C, et al. (2014) MR-sequences for prostate cancer diagnostics: validation based on the PI-RADS scoring system and targeted MR-guided in-bore biopsy. Eur Radiol 24:2582–2589. doi:10.1007/s00330-014-3276-9
11. Shimofusa R, Fujimoto H, Akamata H, et al. (2005) Diffusion-weighted imaging of prostate cancer. J Comput Assist Tomogr 29:149–153
12. Dickinson L, Ahmed HU, Allen C, et al. (2011) Magnetic resonance imaging for the detection, localisation, and characterisation of prostate cancer: recommendations from a European consensus meeting. Eur Urol 59:477–494. doi:10.1016/j.eururo.2010.12.009
13. Barentsz JO, Richenberg J, Clements R, et al. (2012) ESUR prostate MR guidelines 2012. Eur Radiol 22:746–757. doi:10.1007/s00330-011-2377-y
14. Rosenkrantz AB, Kim S, Lim RP, et al. (2013) Prostate cancer localization using multiparametric MR imaging: comparison of Prostate Imaging Reporting and Data System (PI-RADS) and Likert scales. Radiology 269(2):482–492. doi:10.1148/radiol.13122233
15. Röthke M, Blondin D, Schlemmer H-P, Franiel T (2013) PI-RADS classification: structured reporting for MRI of the prostate. RöFo Fortschritte Auf Dem Geb Röntgenstrahlen Nukl 185:253–261. doi:10.1055/s-0032-1330270
16. Heidenreich A, Bastian PJ, Bellmunt J, European Association of Urology, et al. (2014) EAU guidelines on prostate cancer. Part 1: screening, diagnosis, and local treatment with curative intent-update 2013. Eur Urol 65:124–137
17. Epstein JI, Jr Allsbrook WC, Amin MB, ISUP grading committee, et al. (2005) The 2005 International Society of Urological Pathology (ISUP) consensus conference on Gleason grading of prostatic carcinoma. Am J Surg Pathol 29(9):1228–1242
18. Tamada T, Kanomata N, Sone T, et al. (2014) High b value (2,000 s/mm^2) diffusion-weighted magnetic resonance imaging in prostate cancer at 3 Tesla: comparison with 1,000 s/mm^2 for tumor conspicuity and discrimination of aggressiveness. PLoS ONE 9:e96619. doi:10.1371/journal.pone.0096619
19. Kim TH, Jeong JY, Lee SW, et al. (2015) Diffusion-weighted magnetic resonance imaging for prediction of insignificant prostate cancer in potential candidates for active surveillance. Eur Radiol 25:1786–1792. doi:10.1007/s00330-014-3566-2
20. Arumainayagam N, Ahmed HU, Moore CM, et al. (2013) Multi-parametric MR imaging for detection of clinically significant prostate cancer: a validation cohort study with transperineal template prostate mapping as the reference standard. Radiology 268:761–769. doi:10.1148/radiol.13120641
21. Thompson JE, Moses D, Shnier R, et al. (2014) Multiparametric magnetic resonance imaging guided diagnostic biopsy detects significant prostate cancer and could reduce unnecessary biopsies and over detection: a prospective study. J Urol 192:67–74. doi:10.1016/j.juro.2014.01.014
22. Woodfield CA, Tung GA, Grand DJ, et al. (2010) Diffusion-weighted MRI of peripheral zone prostate cancer: comparison of tumor apparent diffusion coefficient with Gleason score and percentage of tumor on core biopsy. AJR Am J Roentgenol 194:W316–W322. doi:10.2214/AJR.09.2651
23. Hambrock T, Somford DM, Huisman HJ, et al. (2011) Relationship between apparent diffusion coefficients at 3.0-T MR imaging and Gleason grade in peripheral zone prostate cancer. Radiology 259:453–461. doi:10.1148/radiol.091409
24. Tanimoto A, Nakashima J, Kohno H, et al. (2007) Prostate cancer screening: the clinical value of diffusion-weighted imaging and dynamic MR imaging in combination with T2-weighted imaging. J Magn Reson Imaging 25:146–152. doi:10.1002/jmri.20793
25. Boesen L, Chabanova E, Løgager V, et al. (2014) Apparent diffusion coefficient ratio correlates significantly with prostate cancer Gleason score at final pathology. J Magn Reson Imaging. doi:10.1002/jmri.24801
26. Thörmer G, Otto J, Horn L-C, et al. (2015) Non-invasive estimation of prostate cancer aggressiveness using diffusion-weighted MRI and 3D proton MR spectroscopy at 3.0 T. Acta Radiol 56:121–128. doi:10.1177/0284185113520311